ENERGY CASCADE AND VORTEX STRUCTURE IN TURBULENT CHANNEL FLOW

Fujihiro Hamba

Institute of Industrial Science
The University of Tokyo
Komaba, Meguro-ku, Tokyo 153-8505, Japan
hamba@iis.u-tokyo.ac.jp

ABSTRACT

The energy transfer in the scale space was examined using the DNS data of turbulent channel flow. The inverse cascade of the spanwise part of turbulent energy was seen near the wall. In order to understand the flow structure associated with the inverse cascade, the conditional average of velocity field was evaluated in relation to the negative value of the energy production term. Profiles of the conditionally averaged quantities showed a large streamwise vortex near the region of the negative production and a small vortex located upstream. It is suggested that the rotation of the former main vortex is driven by the SGS effect under the influence of the latter upstream vortex.

INTRODUCTION

In order to obtain a better understanding of inhomogeneous turbulent flow, it must be useful to examine the energy transfer in the scale space. The scale space for inhomogeneous turbulence corresponds to the wavenumber space for homogeneous turbulence. The second-order velocity structure function $\langle \delta u_i^2 \rangle$ ($\delta u_i = u_i'(\mathbf{x}+\mathbf{r}) - u_i'(\mathbf{x})$) can be considered the energy in the scale space; its transfer has been investigated in detail in the turbulent channel flow (Cimarelli et al. 2013, Cimarelli et al. 2016). Using the two-point velocity correlation $Q_{ii}(\mathbf{r})$ ($= \langle u_i'(\mathbf{x}) u_i'(\mathbf{x}+\mathbf{r}) \rangle$), the author proposed the energy density in the scale space (Hamba 2015, 2018). We also examined the energy density in the turbulent channel flow and investigated the energy transfer in the scale space. The inverse energy cascade, or the transfer from the small to large scales, was seen in some part of the scale space. However, it is not clear what kind of flow structure is accompanied with the inverse cascade.

The vortex structure near the wall in wall-bounded flows has been studied in detail. For example, hair-pin vortex structures have been examined in experiment and numerical simulations. Not only the vortex structures were examined in the snapshot of turbulent field, but also the structures were extracted using the conditional average corresponding to the eject phenomena (ex. Adrian 2007). The self-sustainment mechanisms of the streamwise vortices were also proposed (Waleffe 1997). The mechanism consists of three processes: the streamwise vortices create the streak structure with the aid of the mean shear, the instability of the streak structure generates three-dimensional velocity fluctuations, and the nonlinear effects of the three-dimensional fluctuations generate the streamwise vortices. From the energy point of view, the first and second processes correspond to the forward energy cascade whereas the third one to the inverse cascade.

In this study, we focus on the inverse cascade seen near the wall in the turbulent channel flow and investigate the flow structure associated with the cascade. In particular, we extract the vortex structure by using the conditional average corresponding to the negative energy production in order to examine the relationship between the energy cascade and the vortex structure near the wall in channel flow.

ENERGY TRANSFER IN SCALE SPACE

Using the DNS data of channel flow we examine the energy transfer in the scale space and vortex structures. The DNS was carried out as follows. The Reynolds number of the channel flow is $\mathrm{Re}_\tau = 590$ and computational domain is $L_x \times L_y \times L_z = 2\pi \times 2 \times \pi$. The number of grid points is $N_x \times N_y \times N_z = 1024 \times 192 \times 1024$. Physical quantities are nondimensionalized by the friction velocity u_τ and the channel half width $L_y / 2$. The periodic boundary conditions are used in the streamwise (x) and spanwise (z) directions and the no-slip conditions are imposed at the wall at $y = -1, 1$. We use the fourth-order finite-difference scheme in the x and z directions, the second-order one in the y direction, and the Adams-Bashforth method for time marching. Ensemble average $\langle \ \rangle$ is taken over x-z plane and time period $70 \le t \le 100$.

Using the two-point velocity correlation $Q_{ij}(\mathbf{r})$, the energy density in the scale space in the streamwise direction can be defined as follows:

$$E_{\alpha\alpha}(y, r_x) = -\frac{\partial}{\partial r_x} E_{\alpha\alpha}^>(y, r_x) \qquad (1)$$

where

$$E_{ij}^>(y, r_x) = \int_{-\infty}^{\infty} d\xi_x Q_{ij}(y, \xi_x) G(\xi_x, r_x) \qquad (2)$$

$$G(\xi, r) = \frac{1}{\sqrt{2\pi}r} \exp\left(-\frac{\xi^2}{2r^2}\right) \qquad (3)$$

Summation convention is adopted for repeated indices except for the Greek ones.

The energy transfer term in the scale space appearing in the transport equation for the energy density $E_{\alpha\alpha}(y, r_x)$ is given by

$$\Pi_{\alpha\alpha}(y, r_x)$$
$$= -\int_{-\infty}^{\infty} d\xi_x G(\xi_x, r_x) \frac{\partial}{\partial \xi_k} \langle (u_k'(\mathbf{x} + \boldsymbol{\xi}) - u_k'(\mathbf{x})) u_\alpha'(\mathbf{x}) u_\alpha'(\mathbf{x} + \boldsymbol{\xi}) \rangle \quad (4)$$

Among the three parts of the energy, the transfer of the streamwise part, Π_{xx}, and that of the wall-normal part, Π_{yy}, are negative, representing the forward cascade from the large to small scales. In contrast, the transfer of the spanwise part, Π_{zz}, shows positive values near the wall as plotted in Fig. 1. This positive value represents the inverse cascade; that is, the flux of the energy E_{zz} from the small to large scales.

It was known that the energy $E_{\alpha\alpha}^{>}$ given by (2) is equal to the grid scale (GS) energy $\langle \overline{u}_\alpha'^2 \rangle$ where the filtered velocity is defined as

$$\overline{u}_i(\mathbf{x}) = \int_{-\infty}^{\infty} dx' u_i(\mathbf{x} + x'\mathbf{e}_x) \frac{\sqrt{6}}{\sqrt{\pi}\Delta_x} \exp\left(-\frac{6x^2}{\Delta_x^2}\right) \quad (5)$$

and its filter width is $\Delta_x = \sqrt{6} r_x$ (Hamba 2018). Therefore, the positive value of the transfer Π_{zz} represents the energy transfer from the subgrid scale (SGS) energy to the GS energy. In the following sections we will examine the flow structure at the position $y = -0.975$ ($y^+ = 14.7$) and at the scale $r_x = 0.13$ ($\Delta_x = 0.32$) where the contour of Π_{zz} shows its peak in Fig. 1.

PRODUCTION AND CONDITIONAL AVERAGE

The energy transfer Π_{zz} in the scale space is related to the production term P_{zz} of the SGS energy as follows:

$$\Pi_{zz} = -\langle P_{zz} \rangle, \quad P_{zz} = -2\tau_{zk}\frac{\partial \overline{u}_z}{\partial x_k} \quad (6)$$

where $\tau_{ij} = \overline{u_i u_j} - \overline{u}_i \overline{u}_j$. Since the energy transfer Π_{zz} is an ensemble-averaged quantity, it cannot be directly used to explore the flow structure. Instead of Π_{zz}, we examine the production term P_{zz} to investigate the flow structure.

The production term P_{zz} consists of three parts as follows:

$$P_{zz} = P_{zz1} + P_{zz2} + P_{zz3} \quad (7)$$

$$P_{zz1} = -2\tau_{zx}\frac{\partial \overline{u}_z}{\partial x}, \quad P_{zz2} = -2\tau_{zy}\frac{\partial \overline{u}_z}{\partial y}, \quad P_{zz3} = -2\tau_{zz}\frac{\partial \overline{u}_z}{\partial z} \quad (8)$$

The average of each part at $y^+ = 14.7$ is $\langle P_{zz1} \rangle = -2.48$, $\langle P_{zz2} \rangle = -1.11$, $\langle P_{zz3} \rangle = -4.22$ and the value of $\langle P_{zz3} \rangle$ is the largest. Moreover, the histogram of each part shows that the contribution from P_{zz3} is the largest among the three parts. From the definition of P_{zz3} given by (8), we can see that the negative production P_{zz3} is caused by the positive velocity gradient $\partial \overline{u}_z/\partial z$ because $\tau_{zz} \geq 0$.

We can examine profiles of $\overline{u}_i$ at some locations where P_{zz} is negative in several snapshots. However, it is not clear whether such flow structures are universal or not. In this work, we try to extract the flow structure associated with negative production using the method of conditional average (Adrian 2007). As the conditions, we consider the value of the production term P_{zz}. We set the following condition

$$-100.05 < P_{zz}(x_0, y_0 = -0.975, z_0) < -99.95 \quad (9)$$

to define the conditional average $\langle \ \rangle_{c1}$. We first obtain the combinations of (x_0, z_0) satisfying Eq. (9) from the DNS data of 150 time steps. We then average the local flow fields

$\overline{u}_i(x_0 + \Delta x, y, z_0 + \Delta z)$ around (x_0, z_0) to obtain the conditional average $\langle \overline{u}_i \rangle_{c1}(\Delta x, y, \Delta z)$.

Figures 2 and 3 show the contour plots of the conditional averages $\langle \overline{u}_y \rangle_{c1}$ and $\langle \overline{u}_z \rangle_{c1}$ in the $\Delta z - y$ plane at $\Delta x = 0$, respectively. The gray lines denote the location of $y^+ = 14.7$ ($y = -0.975$). In Fig. 2 the downward flow is clearly seen at $\Delta z = 0$. In Fig. 3 the positive velocity gradient $\partial \overline{u}_z/\partial z$ is seen at $\Delta z = 0$ and $y^+ = 14.7$ representing the diverging flow in the spanwise direction. Therefore, the downward flow creates the spanwise diverging flow because of the impingement to the wall, resulting the increase of the energy $\langle \overline{u}_z'^2 \rangle$. Figure 4 shows the contour plots of the conditional average of the production $\langle P_{zz} \rangle_{c1}$ in the $\Delta z - y$ plane at $\Delta x = 0$. The production is clearly negative at $\Delta z = 0$ and $y^+ = 14.7$. The negative production corresponds to the increase of the GS energy $\langle \overline{u}_z'^2 \rangle$.

In order to understand three-dimensional structure, we plot the isosurfaces of the second invariant of the conditionally averaged velocity $\overline{Q}_{c1}[= -(\partial \langle \overline{u}_i \rangle_{c1}/\partial x_j)(\partial \langle \overline{u}_j \rangle_{c1}/\partial x_i)/2]$ ($=150$) in yellow and that of the production term $\langle P_{zz} \rangle_{c1}$ ($=-50$) in blue in Fig. 5. The positive second invariant shows two streamwise vortices and the negative production region is located just below the two vortices. Because of the impingement to the wall, the downward flow generates the spanwise velocity component and enhances the streamwise vortices.

ANOTHER DEFINITION OF PRODUCTION

The figures shown in the preceding section suggest that the impinging motion is related to the third process of the generation of the streamwise vortex mentioned in the introduction. However, there are some ambiguous points in this interpretation. First, the impinging motion seems to be associated with the energy transfer between the GS energies rather than that from the SGS to GS energies. Second, two streamwise vortices rotating in the opposite direction to each other shown in Fig. 5 are not often observed in snapshots of the DNS data.

With regard to the first point, we can simply understand that the impinging motion representing the transfer from the downstream velocity $\overline{u}_y$ to the spanwise velocity $\overline{u}_z$ because of the wall. This transfer seems to represent the energy transfer between the GS components. The production term P_{zz} given by (6) can be divided into the isotropic part P_{Izz} and the anisotropic part P_{Azz} as follows:

$$P_{zz} = P_{Izz} + P_{Azz}, \quad P_{Izz} = -\frac{2}{3}\tau_{kk}\frac{\partial \overline{u}_z}{\partial z}, \quad P_{Azz} = -2\tau_{zk}^*\frac{\partial \overline{u}_z}{\partial x_k} \quad (10)$$

where $\tau_{ij}^* = \tau_{ij} - (1/3)\tau_{kk}\delta_{ij}$. In the transport equation for the GS energy $\overline{u}_z^2$, the corresponding term $-P_{zz}$ appears as the dissipation due to the SGS effect. However, it is more appropriate to view the isotropic part $-P_{Izz}$ as the energy redistribution among the three parts $\overline{u}_x^2$, $\overline{u}_y^2$, and $\overline{u}_z^2$ because $P_{Ixx} + P_{Iyy} + P_{Izz} = 0$. This suggests that it is better to examine the anisotropic part P_{Azz} rather than P_{zz} as the net production term for the SGS energy τ_{zz}.

Similar to P_{zz}, the anisotropic production term P_{Azz} consists of three parts as follows:

$$P_{Azz} = P_{Azz1} + P_{Azz2} + P_{Azz3} \quad (11)$$

$$P_{Azz1} = -2\tau_{zx}^*\frac{\partial \overline{u}_z}{\partial x}, \quad P_{Azz2} = -2\tau_{zy}^*\frac{\partial \overline{u}_z}{\partial y}, \quad P_{Azz3} = -2\tau_{zz}^*\frac{\partial \overline{u}_z}{\partial z} \quad (12)$$

The average of each part at $y^+ = 14.7$ is $\langle P_{Azz1} \rangle = -2.48$, $\langle P_{Azz2} \rangle = -1.11$, $\langle P_{Azz3} \rangle = 0.11$ and the value of $\langle P_{Azz1} \rangle$ is the

largest as the negative contribution. In contrast to the original production case, the derivative $\partial \overline{u}_z / \partial x$ is important.

With regard to the second point, streamwise vortices with positive streamwise vorticity $\omega_x > 0$ and negative streamwise vorticity $\omega_x < 0$ occur equally in the statistical sense. In Fig. 5, the two vortices are superimposed in the profile of $\langle \overline{u}_i \rangle_{c1}$ because the condition is symmetric with respect to the plane at $\Delta z = 0$. In order to resolve the degeneracy we need another condition in addition to the production term. Here, adopting the anisotropic production and adding the second condition ,we set the following conditions

$$-100.1 < P_{Azz}(x_0, y_0 = -0.975, z_0) < -99.9 \qquad (13)$$

$$\frac{\partial \overline{u}_z}{\partial x}(x_0, y_0 = -0.975, z_0) > 0 \qquad (14)$$

to define the conditional average $\langle \ \rangle_{c2}$. The second condition is introduced because $\partial \overline{u}_z / \partial x$ is important for P_{Azz}.

Figures 6 and 7 show the contour plots of the conditional averages $\langle \overline{u}_y \rangle_{c2}$ and $\langle \overline{u}_z \rangle_{c2}$ in the $\Delta z - y$ plane at $\Delta x = 0$, respectively. The profiles shown in Figs. 6 and 7 are not symmetric about the center line at $\Delta z = 0$. In contrast to Figs. 2 and 3, only one pair of the positive velocity region and the negative velocity region is seen in Fig. 6 and 7. These profiles suggest one streamwise vortex at this cross section at $\Delta x = 0$. Figure 8 shows the contour plots of the conditional average of the production $\langle P_{Azz} \rangle_{c2}$ in the $\Delta z - y$ plane at $\Delta x = 0$. The profile is not symmetric about $\Delta z = 0$ either. Nevertheless, the magnitude of the production is largest at $\Delta z = 0$ and $y^+ = 14.7$.

We plot the isosurfaces of the second invariant of the conditionally averaged velocity $\overline{Q}_{c2}$ ($= 100$) in yellow and that of the production term $\langle P_{Azz} \rangle_{c2}$ ($= -30$) in blue in Fig. 9. We can see one large streamwise vortex and another small vortex located upstream. This figure reminds us of a series of slightly-tilted streamwise vortices with alternate signs of vorticity. Moreover, the region of the strong negative production plotted in blue is attached to the main vortex. This situation is in contrast to Fig. 5 where the negative production region is located apart from the vortices. In Fig. 9, we can interpret that the rotation is the main vortex is driven by the SGS effect under the influence of the small upstream vortex.

CONCLUSIONS

Using the DNS data of channel flow we examined the energy transfer in the scale space. The inverse cascade of the spanwise energy was seen near the wall. In order to understand the flow structure associated with the inverse cascade, we evaluated the conditional average corresponding to the negative production term of the SGS energy. It was shown that the negative production region is located below the two streamwise vortices. Although the imping motion seems to account for the enhancement of streamwise vortices, there are some ambiguous points in the interpretation. Considering the anisotropic part of the SGS production and adding the second condition, we took another conditional average. As a result, we observed a large streamwise vortex and a small vortex located upstream. we can interpret that the rotation of the former main vortex is driven by the SGS effect under the influence of the latter upstream vortex.

REFERENCES

Cimarelli, A., De Angelis, E., and Casciola C. M., 2013, "Paths of energy in turbulent channel flows", *J. Fluid Mech.*, Vol. 715, pp. 436-451.

Cimarelli, A., De Angelis, E., Jimenez, J., and Casciola C. M., 2016, "Cascades and wall-normal fluxes in turbulent channel flows", *J. Fluid Mech.*, Vol. 796, pp. 417-436.

Hamba, F., 2015, "Turbulent energy density and its transport equation in scale space", *Phys. Fluids*, Vol. 27, p. 085108.

Hamba, F., 2018, "Turbulent energy density in scale space for inhomogeneous turbulence", *J. Fluid Mech.*, Vol. 842, pp. 532-553.

Adrian, R. J., 2007, "Hairpin vortex organization in wall turbulence", *Phys. Fluids*, Vol. 19, p. 041301.

Waleffe, F., 1997, "On a self-sustaining process in shear flows", *Phys. Fluids*, Vol. 9, pp. 833-900.
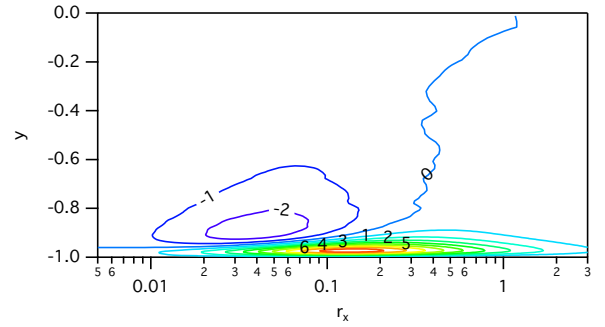
Figure 1. Contour plots of energy flux in the sale space $\Pi_{zz}(y, r_x)$ in the $r_x - y$ plane.
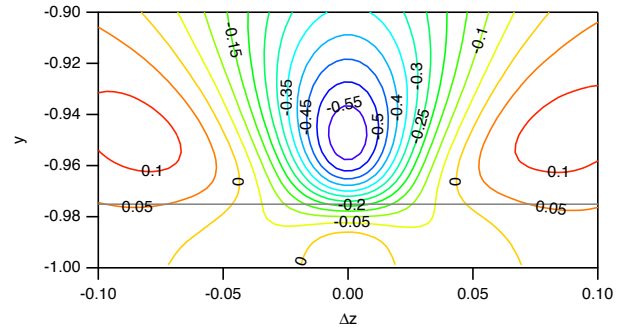
Figure 2. Contour plots of conditional average $\langle \overline{u}_y \rangle_{c1}$ in $\Delta z - y$ plane at $\Delta x = 0$.
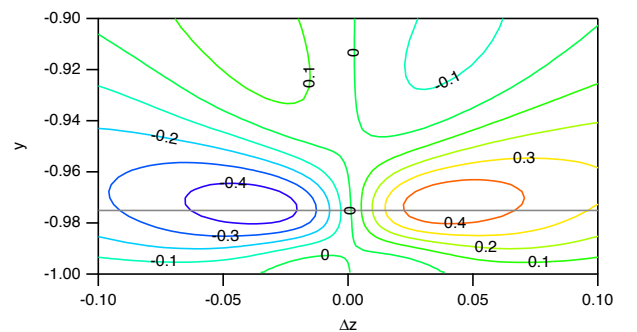
Figure 3. Contour plots of conditional average $\langle \overline{u}_z \rangle_{c1}$ in $\Delta z - y$ plane at $\Delta x = 0$.
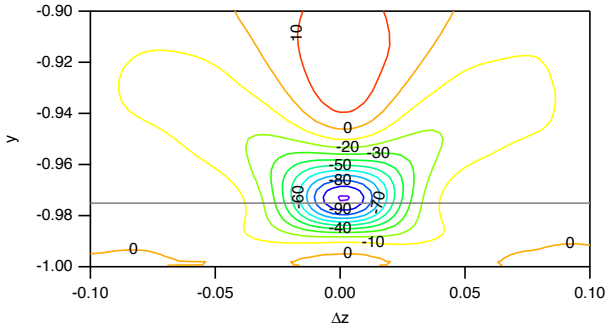
Figure 4. Contour plots of conditional average $\langle P_{zz} \rangle_{c1}$ in $\Delta z - y$ plane at $\Delta x = 0$.
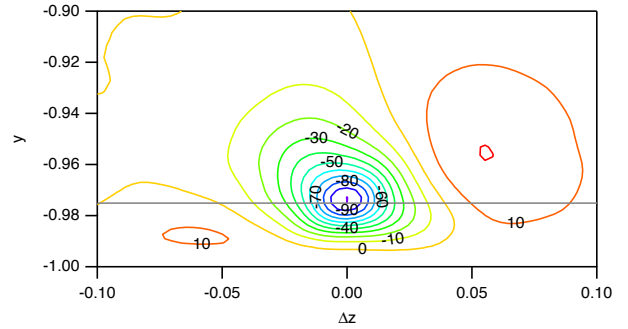
Figure 8. Contour plots of conditional average $\langle P_{Azz} \rangle_{c2}$ in $\Delta z - y$ plane at $\Delta x = 0$.
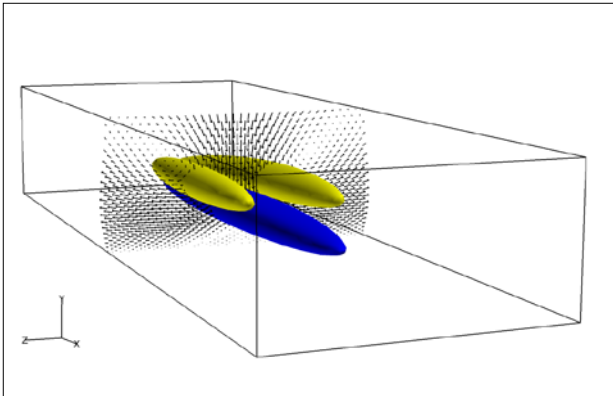
Figure 5. Isosurfaces of conditional averages $\overline{Q}_{c1}$ and $\langle P_{zz} \rangle_{c1}$. The domain is $-0.3 \leq \Delta x \leq 0.3$, $-1 \leq y \leq -0.9$, and $-0.1 \leq \Delta z \leq 0.1$
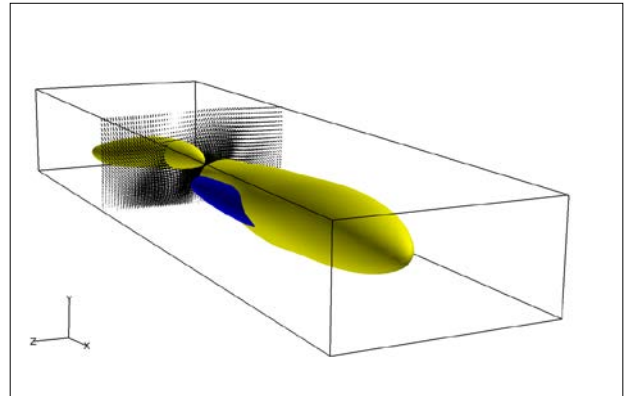
Figure 9. Isosurfaces of conditional averages $\overline{Q}_{c2}$ and $\langle P_{Azz} \rangle_{c2}$. The domain is $-0.37 \leq \Delta x \leq 0.37$, $-1 \leq y \leq -0.9$, and $-0.1 \leq \Delta z \leq 0.1$
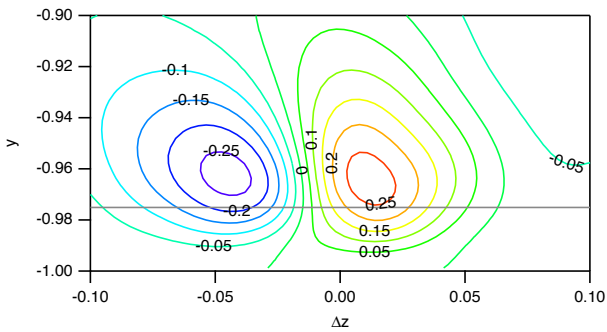
Figure 6. Contour plots of conditional average $\langle \overline{u}_y \rangle_{c2}$ in $\Delta z - y$ plane at $\Delta x = 0$.
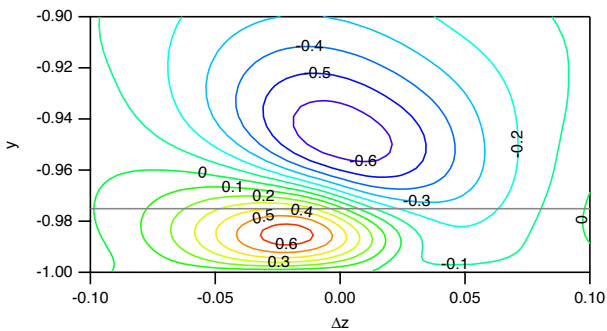
Figure 7. Contour plots of conditional average $\langle \overline{u}_z \rangle_{c2}$ in $\Delta z - y$ plane at $\Delta x = 0$.

4